Runaway electron generation in a cooling plasma

H. Smith
Department of Radio and Space Science, Chalmers University of Technology, SE-412 96 Göteborg, Sweden

P. Helander
Euratom/UKAEA Fusion Association, Culham Science Centre, Abingdon OX14 3DB, United Kingdom

L.-G. Eriksson
Association EURATOM-CEA, CEA/DSM/DRFC, CEA-Cadarache, F-13108 St, Paul lez Durance, France

T. Fülöp
Department of Radio and Space Science, Chalmers University of Technology, SE-412 96 Göteborg, Sweden

(Received 19 September 2005; accepted 4 November 2005; published online 20 December 2005)

The usual calculation of Dreicer [Phys. Rev. **115**, 238 (1959); **117**, 329 (1960)] generation of runaway electrons assumes that the plasma is in a steady state. In a tokamak disruption this is not necessarily true since the plasma cools down quickly and the collision time for electrons at the runaway threshold energy can be comparable to the cooling time. The electron distribution function then acquires a high-energy tail which can easily be converted to a burst of runaways by the rising electric field. This process is investigated and simple criteria for its importance are derived. If no rapid losses of fast electrons occur, this can be a more important source of runaway electrons than ordinary Dreicer generation in tokamak disruptions. © *2005 American Institute of Physics*. [DOI: 10.1063/1.2148966]

I. INTRODUCTION

Runaway electron generation is common in tokamak disruptions and poses a possible threat to a next-step device. As the plasma cools down quickly in the thermal quench of a disruption, a large toroidal electric field is induced which accelerates some electrons to relativistic energies. These electrons may severely damage the first wall on impact.

Such acceleration of an electron occurs if its velocity exceeds a critical speed, above which the friction force from collisions with other plasma particles becomes smaller than the force from the electric field. An electron can enter this "runaway" region in velocity space either as a result of a random walk with many small steps taken in velocity space (caused by long-range Coulomb collisions), or through a sudden collision at a close range that throws it above the critical speed in a single event. The former of these mechanisms was the first to be investigated[1,2] and is usually referred to as "Dreicer" runaway generation. The latter mechanism is important in tokamaks with large plasma current and is referred to as a runaway avalanche.[3]

The usual analysis of these processes presumes that the plasma is in a quasisteady state—an assumption that is likely to fail if the duration of the thermal quench is shorter than the collision time for electrons near the runaway threshold energy. In this case, sufficiently energetic electrons do not have time to cool down and equilibrate with the Maxwellian bulk. Instead, they will form a high-energy tail and the number of electrons in the runaway region will be enhanced. This has been observed in numerical simulations of pellet injection into high-temperature plasmas, and results in a burst of runaway electron generation.[4,5] It has also been borne out in experiments with high-Z "killer" pellet quenching in DIII-D.[6] The size of the runaway burst depends sensitively on the rate at which the cooling takes place and the final temperature of the plasma.

The purpose of the present paper is to supplement the numerical simulations of runaway burst generation in Refs. 4 and 5 by investigating this process in greater mathematical detail and to derive simple but approximate criteria for whether it is important. This is accomplished by solving the electron kinetic equation in a rapidly cooling plasma along the lines laid out in Ref. 7 and estimating the number of electrons in the runaway region. The specific solution constructed in Ref. 7 is extended to allow for electron-density variation, and is also supplemented by numerical solutions allowing a more general temperature variation.

The results are potentially applicable to several plasma termination scenarios. Controlled plasma shutdown may be achieved either by killer pellets or by massive gas injection,[6,8] and runaway bursts can in principle occur during both. Our results are also applicable to spontaneous disruptions insofar as no preferential losses of fast electrons occur. It is believed that the thermal quench in a disruption occurs both as a result of heat conduction to the wall and by radiative cooling due to an influx of impurities. Our analysis pertains to the latter case rather than the first, which would certainly involve fast electron losses. It has been suggested that the first stage of the thermal quench is due to heat conduction and the second to radiation.[9] A runaway burst could then occur in the second stage.

The structure of the paper is the following: In Sec. II the kinetic equation is formulated, and Sec. III shows how the runaway electron density can be estimated from its solution.

In Sec. IV the particular analytical solution derived in Ref. 7 is recalled, and its implications for runaway generation are discussed. These results are compared in Sec. V with numerical solutions, and in Sec. VI the effect of electron-density variation is investigated. Finally, our conclusions are summarized in Sec. VII.

II. FOKKER-PLANCK EQUATION FOR ELECTRONS

The analysis is based on the kinetic equation for electrons in an electric field $E_\parallel$,

$$\frac{\partial f}{\partial t} + \frac{eE_\parallel}{m_e}\left(\xi\frac{\partial f}{\partial v} + \frac{1-\xi^2}{v}\frac{\partial f}{\partial \xi}\right) = C_e(f), \tag{1}$$

where $\xi = v_\parallel/v = \cos\theta$ is the cosine of the pitch angle and $v_\parallel$ is positive in the direction in which electrons are accelerated by $E_\parallel$. The Fokker-Planck collision operator for electrons colliding with a Maxwellian background is[10]

$$C_e(f) = \hat{\nu}_{ee} v_T^3 \left[\frac{1+Z}{v^3}\mathcal{L}(f) + \frac{1}{v^2}\frac{\partial}{\partial v} 2G\left(\frac{v}{v_T}\right)\left(\frac{v^2}{v_T^2}f + \frac{v}{2}\frac{\partial f}{\partial v}\right)\right], \tag{2}$$

where

$$\mathcal{L} = \frac{1}{2}\frac{\partial}{\partial \xi}(1-\xi^2)\frac{\partial}{\partial \xi} \tag{3}$$

is the Lorentz scattering operator, $v_T(t) = (2T(t)/m_e)^{1/2}$ is the electron thermal velocity, $\hat{\nu}_{ee}(t) = ne^4 \ln\Lambda/4\pi\epsilon_0^2 m_e^2 v_T^3(t)$ is the thermal collision frequency, n and T denote the electron density and temperature, respectively, and $G(x)$ is the Chandrasekhar function

$$G(x) = \frac{\mathrm{erf}(x) - x\,\mathrm{erf}'(x)}{2x^2}. \tag{4}$$

It is convenient to introduce the normalized velocity $x = v/v_T$ and the normalized distribution function

$$F = \frac{\pi^{3/2} v_T^3}{n} f, \tag{5}$$

so that a Maxwellian distribution is represented by $F = e^{-x^2}$ and the kinetic equation becomes

$$\frac{1}{\hat{\nu}_{ee}}\frac{\partial F}{\partial t} + \epsilon\left(\xi\frac{\partial F}{\partial x} + \frac{1-\xi^2}{x}\frac{\partial F}{\partial \xi}\right) + \delta\left(3F + x\frac{\partial F}{\partial x}\right) = \frac{1+Z}{x^3}\mathcal{L}(F) + \frac{1}{x^2}\frac{\partial}{\partial x} 2x^2 G(x)\left(F + \frac{1}{2x}\frac{\partial F}{\partial x}\right), \tag{6}$$

where

$$\epsilon(t) = \frac{eE_\parallel}{m_e v_T \hat{\nu}_{ee}} \tag{7}$$

and

$$\delta(t) = -\frac{1}{2T\hat{\nu}_{ee}}\frac{dT}{dt}. \tag{8}$$

The two terms in Eq. (6) that are proportional to δ appear because of the time-dependent normalizations of the velocity and the distribution function.

III. RUNAWAY ELECTRON GENERATION

The critical velocity above which electron runaway occurs is[11]

$$v_c = v_T\sqrt{\frac{E_D}{2E_\parallel}}, \tag{9}$$

where $E_D = ne^3 \ln\Lambda/4\pi\epsilon_0^2 T$ is the Dreicer field and $\ln\Lambda$ is the Coulomb logarithm. On the short time scale of the thermal quench (less than 1 ms in a typical disruption), the plasma inductance prevents the parallel plasma current from changing. Since the Spitzer resistivity $\eta_\parallel$ is proportional to $T^{-3/2}$,[10] one also expects the electric field $E_\parallel = \eta_\parallel j_\parallel$ to be proportional to $T^{-3/2}$, as long as the current carried by the runaway electrons is negligible. Assuming that the electron density is constant in time, this results in the normalized critical velocity

$$x_c(t) = \frac{v_c}{v_T} = \sqrt{\frac{E_{D0}}{2E_{\parallel 0}}}\left(\frac{T(t)}{T_0}\right)^{1/4}, \tag{10}$$

where the subscript 0 denotes the initial value of the corresponding quantities. (The effect of increasing density during the disruption is investigated in Sec. VI.) It is the fact that x_c decreases with time in a cooling plasma that makes runaway generation relatively easy in a disruption.

If the plasma cools down so quickly that electrons with velocities exceeding x_c do not have time to thermalize, a high-energy tail forms in the distribution function and the number of electrons in the runaway region is enhanced. This results in the "burst" of runaway production discussed in the Introduction. To obtain approximations for the number of runaways in the burst, we will neglect the influence of $E_\parallel$ on the distribution function f, and investigate how the tail of f develops under the influence of collisions when the temperature falls rapidly. When the electric field is neglected, the distribution function remains isotropic in velocity space, whereas a tail is pulled out in the direction of $v_\parallel$ if the electric field is retained. Nevertheless, the neglect of the electric field has a surprisingly small effect on the number of tail particles in a cooling plasma, as will be shown by full numerical simulations in Sec. V.

In the absence of an electric field, the pitch-angle dependence can be neglected in the kinetic equation (6), which then simplifies to

$$\frac{1}{\hat{\nu}_{ee}}\frac{\partial F}{\partial t}+\delta\left(3F+x\frac{\partial F}{\partial x}\right)=\frac{1}{x^2}\frac{\partial}{\partial x}2x^2G(x)\left(F+\frac{1}{2x}\frac{\partial F}{\partial x}\right). \tag{11}$$

This equation has been solved numerically and analytically for different time evolutions of the electron temperature, using a Maxwellian distribution as an initial condition and $\partial F/\partial x=0$ at $x=0$ and $F(x)\to 0$ for $x\to\infty$ as boundary conditions. The results are presented in Secs. IV and V.

When Eq. (11) has been solved and $F(x,t)$ is known, the number of particles inside the runaway region of velocity space can be determined. If velocity diffusion is neglected in the kinetic equation, there is a sharp separatrix between the thermal and runaway regions. This separatrix is given by the orbit through the point $\xi=1$, $v=v_c$, which if $x_c\gg 1$ is determined by the equations

$$\frac{dv}{dt}=-\hat{\nu}_{ee}\frac{v_T^3}{v^3}v+\frac{eE_\parallel}{m_e}\xi, \tag{12}$$

$$\frac{d\xi}{dt}=\frac{eE_\parallel}{m_e}\frac{1-\xi^2}{v}, \tag{13}$$

or

$$\frac{dx}{d\xi}=\frac{\xi-x_c^2/x^2}{1-\xi^2}x, \tag{14}$$

so that the separatrix becomes

$$\xi_{\mathrm{sep}}(x)=2\frac{x_c^2}{x^2}-1. \tag{15}$$

The number of particles n_{run} inside the runaway region can now be estimated as

$$\begin{aligned}n_{\mathrm{run}}&=\int_{v_c}^{\infty}\int_0^{\theta_{\mathrm{sep}}(v)}\int_0^{2\pi}fv^2\sin\theta d\varphi d\theta dv\\&=2\pi\int_{v_c}^{\infty}(1-\xi_{\mathrm{sep}})fv^2dv=\frac{4}{\sqrt{\pi}}n\int_{x_c}^{\infty}F(x^2-x_c^2)dx.\end{aligned} \tag{16}$$

The result will be compared with the usual formula for primary generation, assuming that the ion charge $Z=1$, cf. Ref. 2,

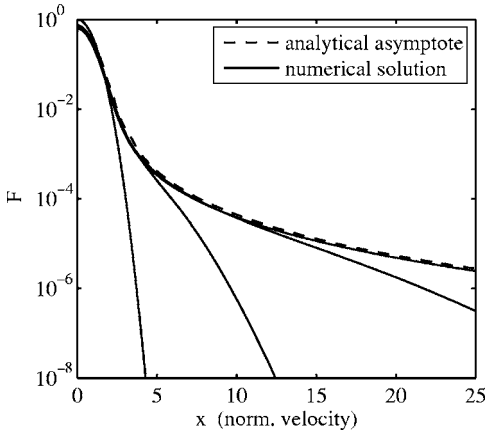

FIG. 1. (Dashed) the analytical asymptotic distribution function (19) as $t\to t_0$ for $\delta=0.05$, which is typical of a JET disruption. (Solid) a numerical solution given at the times corresponding to the temperatures $T/T_0=1$, 10^{-1}, 10^{-2}, and 10^{-3} (from left to right).

$$\frac{dn_{\mathrm{run}}}{dt}=kn\hat{\nu}_{ee}\left(\frac{E_{\mathrm{D}}}{E_\parallel}\right)^{3/8}e^{-E_{\mathrm{D}}/4E_\parallel-\sqrt{2E_{\mathrm{D}}/E_\parallel}}, \tag{17}$$

where k is a factor of order unity. For a Maxwellian distribution function, these two expressions are in reasonably good agreement for typical values of $E_{\mathrm{D}}/E_\parallel$, as will be seen below.

IV. ANALYTICAL SOLUTION OF THE KINETIC EQUATION WHEN δ=CONST

In the early stages of the thermal quench phase of a tokamak disruption the differential cross sections for excitation and ionization by electron impact are inversely proportional to the electron energy in the Born approximation where this energy far exceeds the relevant thresholds.[12] If the impurity content is constant, this leads to an energy-loss rate from the plasma proportional to $T^{-1/2}$, so that the temperature evolution is approximately expected to follow

$$T(t)=T_0(1-t/t_0)^{2/3}. \tag{18}$$

In the notation of Eq. (11) this corresponds to constant δ, and a temperature decay time $t_0=1/(3\nu_0\delta)$, where $\nu_0\equiv\hat{\nu}_{ee}(0)$ is the initial thermal collision frequency. For this particular cooling history, Eq. (11) can be solved analytically[7] by expanding in the smallness of the parameter δ, assuming that the plasma cooling time is smaller than the thermal collision time. This gives an asymptotic distribution function when $T\to 0$ at the time t_0 as

$$\lim_{t\to t_0}F(y,t)=\begin{cases}\exp\left[-\delta^{-2/3}\left(y^2-\dfrac{2y^5}{5}\right)\right], & \delta^{1/3}\ll y<1\\ \dfrac{1}{2}\exp\left\{3\delta^{-2/3}\left[(y-1)^2-\dfrac{1}{5}\right]\right\}\mathrm{erfc}[\sqrt{3}(y-1)\delta^{-1/3}], & y-1\sim\delta^{1/3}\\ \sqrt{\dfrac{3}{\pi}}\dfrac{\delta^{1/3}}{2}\exp\left(-\dfrac{3}{5\delta^{2/3}}\right)\dfrac{1}{y^3-1}, & y>1,\end{cases} \tag{19}$$

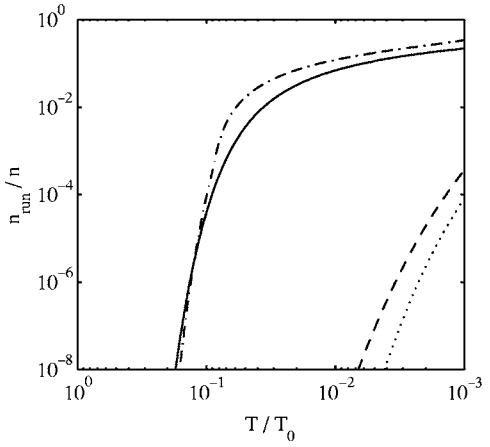

FIG. 2. Comparison of the analytical estimate in Eqs. (20) and (21) for the runaway burst density (dash-dotted) with a numerical evaluation of Eq. (16) (solid), the usual Dreicer production (dashed), and the number of electrons in the runaway region of a Maxwellian (dotted). The estimates are plotted against the instantaneous temperature, which evolves according to Eq. (18). Here $E_{D0}/E_0=530$ and $\delta=0.05$.

where $y=x\delta^{1/3}$. Figure 1 shows how a numerical solution of the kinetic equation (11) approaches the analytical asymptote as $t\rightarrow t_0$.

It was shown in Ref. 7 that when the tail has extended into the region $y>1$, the distribution function follows the asymptote from low velocities up to approximately $x_{\mathrm{tail}}=\delta^{-1/3}\sqrt{T_0/T(t)}$, where it begins to fall off more rapidly, instead following the initial Maxwellian distribution. At early times, $\delta^{-1/3}<x_{\mathrm{tail}}<x_{\mathrm{c}}$, the number of particles in the runaway region can be estimated as

$$\begin{aligned} n_{\mathrm{run}}/n &= \frac{4}{\sqrt{\pi}}\int_{v_c/v_{T0}}^{\infty} e^{-x^2}\left(x^2-\frac{v_c^2}{v_{T0}^2}\right)dx \\ &\simeq \frac{2}{\sqrt{\pi}}\frac{v_{T0}}{v_{\mathrm{c}}}\exp\left(-\frac{v_c^2}{v_{T0}^2}\right) \\ &= \frac{2}{\sqrt{\pi}}\left[\frac{E_{\mathrm{D0}}}{2E_{\|0}}\left(\frac{T}{T_0}\right)^{3/2}\right]^{-1/2}\exp\left[-\frac{E_{\mathrm{D0}}}{2E_{\|0}}\left(\frac{T}{T_0}\right)^{3/2}\right]. \end{aligned} \tag{20}$$

Later, when $\delta^{-1/3}<x_{\mathrm{c}}<x_{\mathrm{tail}}$, the estimate becomes

$$\begin{aligned} n_{\mathrm{run}}/n &= \frac{4}{\sqrt{\pi}}\int_{x_{\mathrm{c}}}^{x_{\mathrm{tail}}} F(x^2-x_c^2)dx \\ &\quad + \frac{4}{\sqrt{\pi}}\int_{v_{\mathrm{tail}}/v_{T0}}^{\infty} e^{-x^2}\left(x^2-\frac{v_c^2}{v_{T0}^2}\right)dx \\ &\simeq \frac{\delta^{-2/3}}{\sqrt{3}\pi}\exp\left(-\frac{3}{5}\delta^{-2/3}\right) \\ &\quad \times\left[2\ln\left(\frac{\delta x_{\mathrm{tail}}^3-1}{\delta x_c^3-1}\right)-3\left(1-\frac{x_c^2}{x_{\mathrm{tail}}^2}\right)\right] \\ &\quad + \frac{2}{\sqrt{\pi}}\delta^{1/3}\exp(-\delta^{-2/3}). \end{aligned} \tag{21}$$

In Fig. 2 the number of runaways produced in the burst, as calculated from the estimate (16) using a numerical solution of Eq. (11), is compared with the analytical estimates from Eqs. (20) and (21). The steep part of the analytical curve in Fig. 2 corresponds to Eq. (20) and the flatter part to Eq. (21). Also shown are the time integral of the Dreicer generation rate (17) and the number of electrons in the runaway region of a Maxwellian, i.e., the estimate (16) applied to a Maxwellian F. The latter is apparently a reasonable approximation to the Dreicer generation rate.

It is evident from the figure that far more runaways are generated in the burst than by the ordinary Dreicer mechanism. In fact, as long as $x_{\mathrm{c}}>\delta^{-1/3}$ the runaway burst always dominates over ordinary Dreicer production, since the distribution function above the runaway threshold is then much larger than a Maxwellian. More explicitly, this inequality corresponds to

$$\delta>\left(\frac{E_{\mathrm{D}}}{2E_{\|}}\right)^{-3/2}, \tag{22}$$

or equivalently

$$\nu_0 t_0<\frac{1}{3}\left(\frac{E_{\mathrm{D}}}{2E_{\|}}\right)^{3/2}. \tag{23}$$

This condition gives a limit on how fast the plasma has to cool down (or if the cooling rate is fixed, how far the temperature is allowed to fall) for the burst to be more significant than Dreicer generation. Relating the parallel electric field to the current density $E_{\|}=\eta_{\|}j_{\|}$ and using $j_{\|}=2B/\mu_0 qR$, where q is the safety factor, we find

$$\frac{E_{\mathrm{D}}}{E_{\|}}\simeq\left(\frac{\pi T}{2m_e}\right)^{1/2}\frac{3\mu_0 enqR}{B}. \tag{24}$$

This ratio is smallest at $T=T_{\mathrm{final}}$ and can be used to estimate the importance of runaway bursts in experiments. For instance, one readily concludes that such bursts could be very important in disruptions in the Joint European Torus (JET).[13] Using the parameters of a typical JET discharge (63133) where a disruption was triggered intentionally (initial temperature $T_0=3.1$ keV, final temperature $T_{\mathrm{final}}=10$ eV, electron density $n_0=3\times10^{19}$ m^{-3}, major radius $R=3$ m, magnetic field $B=3$ T, central safety factor $q=1$, and cooling time $t_0\simeq0.5$ ms), one finds $\nu_0 t_0\simeq5$ while the criterion (23) gives $\nu_0 t_0<20$. Note that $E_{\mathrm{D}}/E_{\|}\simeq30$ and $E_{\mathrm{D}}/E_{\mathrm{c}}=m_e c^2/T=5.1\times10^4$ at $T=T_{\mathrm{final}}$, so that $E_{\|}\gg E_{\mathrm{c}}$.

The projected values for the International Thermonuclear Experimental Reactor[14] (ITER) are $n_0\simeq10^{20}$ m^{-3}, $T_0\simeq20$ keV, $R=6.2$ m, and $B=5.3$ T. Assuming that $T_{\mathrm{final}}=10$ eV, Eq. (24) gives $E_{\mathrm{D}}/E_{\|}\simeq120$ (which again implies that $E_{\|}\gg E_{\mathrm{c}}$) and Eq. (22) yields $\delta>2\times10^{-3}$. The electron collision time becomes $\nu_0^{-1}=0.5$ ms, so the limit for the disruption time is $t_0=1/(3\nu_0\delta)<0.08$ s. This is longer than the expected disruption time (indeed longer than the time separation between the initial and final stages of the thermal quench[15]). Thus, if the temperature follows Eq. (18), the density is constant, and not too many fast electrons are lost from the plasma, then runaway bursting should be highly significant in ITER.

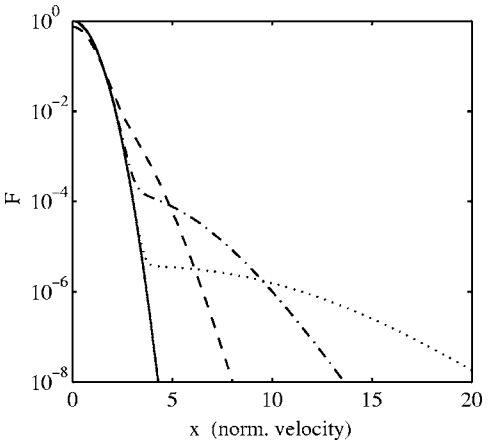

FIG. 3. The distribution function at times 0 ms (solid), 0.25 ms (dashed), 0.5 ms (dash-dotted), and 0.75 ms (dotted). Exponential temperature decay, Eq. (25), has been used together with the parameters $T_0=3.1$ keV, $T_{\text{final}}=10$ eV, and $t_*=0.2$ ms from JET discharge 63133.

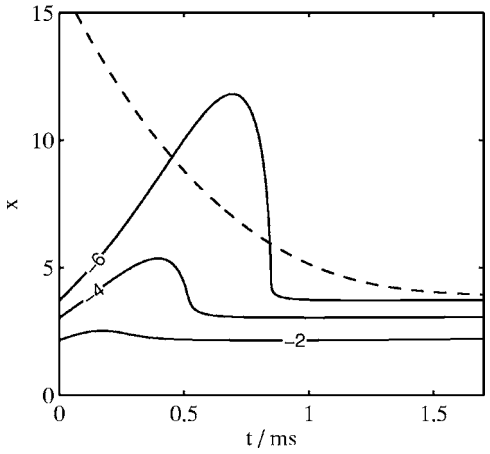

FIG. 4. Contour curves of the same distribution function as in Fig. 3 are shown in solid at the levels of 10^{-2}, 10^{-4}, and 10^{-6}. The dashed curve shows the runaway threshold velocity x_c, calculated from $E_{D0}/E_{\|0}=530$ from JET discharge 63133.

V. NUMERICAL RESULTS

As pointed out at the beginning of Sec. IV, the temperature is only expected to follow Eq. (18) in the early stages of the thermal quench, but since most of the runaway production occurs at low temperatures, it is important to consider other cooling histories than Eq. (18). Only for the particular choice of temperature evolution (18) can the kinetic equation (11) be solved analytically. Otherwise the parameter δ varies in time and it becomes necessary to solve Eq. (11) numerically. This has been accomplished using a finite difference scheme, which has been benchmarked both against the analytically tractable limit (19) in Fig. 1 and against the analysis of runaway electrons by numerical algorithms (ARENA) Monte Carlo code.[16]

As an example, the kinetic equation has been solved assuming an exponential temperature decay,

$$T = T_{\text{final}} + (T_0 - T_{\text{final}})e^{-t/t_*}, \tag{25}$$

which may be a more realistic model than (18) as it results in a cooling rate $\delta(t)$ that decreases with time. A typical solution is presented in Figs. 3–5, where parameters from the previously mentioned JET discharge 63133 are used. Figure 3 shows how remnants of the initial thermal distribution extend to high energies as a tail in the distribution function when the temperature falls. As the runaway threshold velocity x_c, the dashed curve in Fig. 4, decreases it carves out the part of this distribution that becomes the runaway region. The burst of runaways generated this way is compared with the usual Dreicer mechanism in Fig. 5. At the time of the burst, the Dreicer runaway density is very low, but since it continues to produce runaways as the temperature falls further, it may become important at later times. In this case, runaways are thus generated in two stages, first in a burst caused by cooling and later by the usual Dreicer mechanism. If the burst is large enough, it may trigger a secondary avalanche of knock-on runaways rendering any subsequent Dreicer generation unimportant. Alternatively, the burst may modify the toroidal electric field and reduce it below the level where appreciable Dreicer generation can occur.

It is interesting to compare the runaway bursts resulting from the two different types of temperature decay shown in Fig. 6. In the first case the temperature follows Eq. (18) until it reaches a certain final temperature, $T_{\text{final}} \ll T_0$, shortly before the time t_0, and then remains constant. The second case corresponds to Eq. (25), where the final temperature T_{final} is the same as in the first case. For the comparison we choose $t_*=t_0/4$ since this makes the number of runaway particles reach its maximum at approximately the same time. The resulting runaway generation is shown in Fig. 7. Significantly fewer runaways are produced in the case of exponential temperature decay since the parameter δ then decreases with time and is therefore relatively small at the later stages of the cooling when the electric field is largest. It may be concluded that runaway bursts are sensitive to the way in which the temperature decays during the thermal quench, which is poorly diagnosed in experiments.

So far, we have entirely neglected the effect of the electric field on tail formation in the electron distribution function. This field has merely been used to determine the critical velocity delineating the runaway region in velocity space,

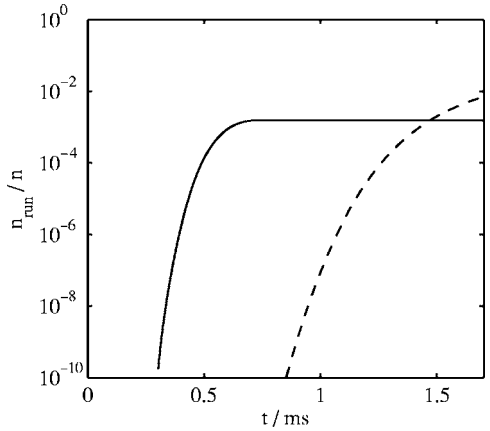

FIG. 5. (Solid) the density of tail electrons in the runaway region calculated for the case in Figs. 3 and 4. (Dashed) the usual Drecier runaway generation, Eq. (17).

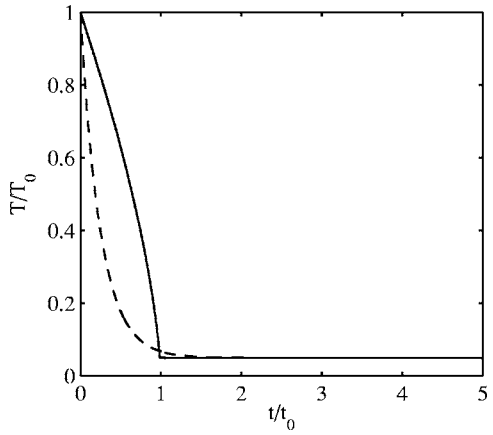

FIG. 6. Two different types of temperature decay with the same final temperature $T_{\text{final}}/T_0=0.05$. (Solid) the temperature follows Eq. (18) until it reaches T_{final} shortly before the time t_0, and then remains constant. (Dashed) the temperature falls exponentially according to Eq. (25) with $t_*=t_0/4$.

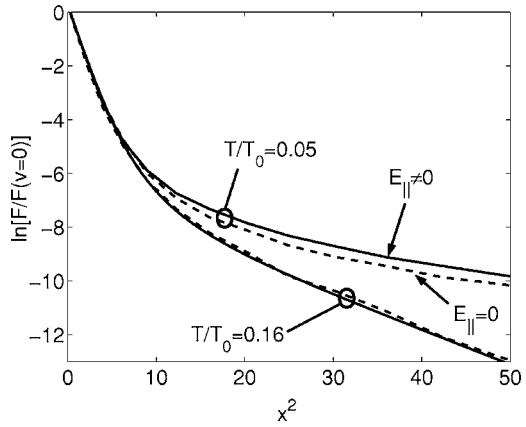

FIG. 8. The solution from the finite difference scheme (lower solid) is benchmarked against the ARENA Monte Carlo simulation (lower dashed) for the case $\delta=0.03$, $T/T_0=0.16$ with no electric field. The upper two curves show the difference between the electron distribution function when the electric field is neglected and the pitch-angle-averaged distribution function when it is retained, as calculated by ARENA for the case $\delta=0.03$, $T_{\text{final}}/T_0=0.05$, and $E_\parallel/E_{\text{D}}=0.03$ at $T=T_{\text{final}}$.

but its direct effect on the distribution function has been neglected. In actual fact, the electric field of course modifies the distribution function by accelerating high-energy electrons in the direction $-e\mathbf{E}$. This makes the distribution anisotropic and also enhances the formation of the high-energy tail. In order to assess the importance of this effect in a cooling plasma, we have used the ARENA Monte Carlo code[16] to calculate the evolution of the distribution function with the electric field taken into account, thus solving the full kinetic equation (1) with the collision operator (2).

Figures 8 and 9 show the result of such simulations with the temperature decay given by Eq. (18) and an electric field reaching $E_\parallel/E_{\text{D}}=0.03$ at the end of the cooling, which is a typical value in JET disruptions. When this field is neglected, the distribution function agrees with that calculated by the code used previously in this section, as shown in Fig. 8. When the field is retained, the tail in the distribution function becomes anisotropic (Fig. 9) and is enhanced above the critical velocity (Fig. 8), as expected. However, as compared with a Maxwellian, this enhancement is much smaller than that already caused by the cooling of the plasma. It thus appears justified to neglect the electric field as done elsewhere in this paper. The electric field is important insofar as it establishes a runaway acceleration region in velocity space, but does not significantly enhance the high-energy tail in a sufficiently rapidly cooling plasma.

VI. THE EFFECT OF INCREASING DENSITY

In disruptions, the electron density is usually not constant throughout the thermal quench but rises because of the ionization of impurities. This has three effects that can decrease the runaway generation. The first effect is related to

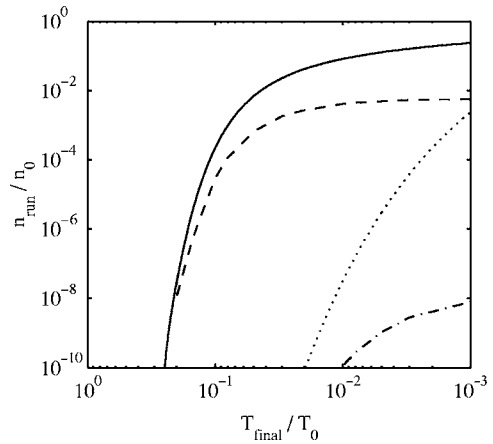

FIG. 7. A comparison between the two types of temperature evolution in Fig. 6. The dashed curve shows the runaway density as a function of the final temperature T_{final}/T_0, when T falls exponentially according to Eq. (25). The runaway production is less efficient than in the temperature evolution with constant δ case (solid). The Dreicer runaway density at the time t_0 is shown for the exponential case (dash-dotted) and the constant δ case (dotted). In this example $\delta=0.05$ and $E_{\text{D0}}/E_{\parallel 0}=400$ was used.

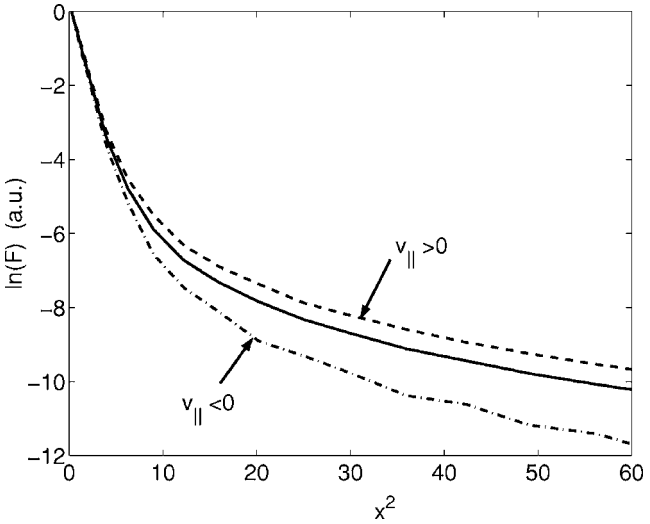

FIG. 9. Anisotropy of the electron distribution function in the ARENA simulation of the case $\delta=0.03$, $T_{\text{final}}/T_0=0.05$, and $E_\parallel/E_{\text{D}}=0.03$ at $T=T_{\text{final}}$. The pitch-angle-averaged distribution function (solid) is compared with the distribution function averaged only over pitch angles with $v_\parallel>0$ (dashed) and over pitch angles with $v_\parallel<0$ (dash-dotted).

the critical electric field. No runaways are produced until $E_\parallel$ exceeds $E_c = E_D T/(m_e c^2)$, which translates into a condition on the density and temperature

$$\frac{n(t)}{n_0}\left[\frac{T(t)}{T_0}\right]^{3/2} < \frac{m_e c^2}{T_0}\frac{E_{\parallel 0}}{E_{D0}}. \tag{26}$$

To have runaway production at T_{final} for the JET example discussed in Sec. IV, one needs $n_{final}/n_0 < 1.7\times 10^3$, and for the ITER example the condition is $n_{final}/n_0 < 450$. The second effect is that the critical velocity changes because of the density dependence of the Dreicer field E_D, so that

$$x_c(t) = \frac{v_c}{v_T} = \sqrt{\frac{E_D}{2E_\parallel}} = \sqrt{\frac{E_{D0}}{2E_{\parallel 0}}}\left[\frac{T(t)}{T_0}\right]^{1/4}\left[\frac{n(t)}{n_0}\right]^{1/2}. \tag{27}$$

The third effect is a higher collision frequency, which reduces the number of particles in the high-energy tail of the distribution. This can be included in our kinetic equation by adding a source term of Maxwellian particles with a very low temperature $\bar{T}$. Demanding $\bar{T} \ll T$ ensures that the source term does not directly introduce new particles into the tail. The source term becomes

$$S(v,t) = \frac{1}{\bar{n}}\frac{d\bar{n}}{dt}\bar{f}(v,t), \tag{28}$$

where

$$\bar{f}(v,t) = \frac{\bar{n}(t)}{\pi^{3/2}\bar{v}_T^3}\exp\left[-\left(\frac{v}{\bar{v}_T}\right)^2\right], \tag{29}$$

and $\bar{v}_T = [2\bar{T}(t)/m_e]^{1/2}$. The new particles added by the source are quickly thermalized by collisions with the bulk population of electrons with temperature T. The collision frequency is $\hat{\nu}_{ee}(t) = n(t)e^4 \ln\Lambda/4\pi\epsilon_0^2 m_e^2 v_T^3(t)$, where $n(t) = n_0 + \bar{n}$ is the total electron density, and the normalized kinetic equation Eq. (11) becomes

$$\frac{1}{\hat{\nu}_{ee}}\frac{\partial F}{\partial t} + (\lambda + 3\delta)F + \delta x\frac{\partial F}{\partial x} = \frac{1}{x^2}\frac{\partial}{\partial x}2x^2 G(x)\left(F + \frac{1}{2x}\frac{\partial F}{\partial x}\right) + \lambda\left(\frac{T}{\bar{T}}\right)^{3/2}\exp\left(-x^2\frac{T}{\bar{T}}\right), \tag{30}$$

where

$$\lambda = \frac{1}{n\hat{\nu}_{ee}}\frac{dn}{dt}. \tag{31}$$

The special case when λ is constant corresponds to the density and temperature evolution

$$n(t) = n_0(1 - t/t_0)^{-\lambda/(3\alpha\delta)}, \tag{32}$$

$$T(t) = T_0(1 - t/t_0)^{2/(3\alpha)}, \tag{33}$$

where $\alpha = 1 + \lambda/(3\delta)$. The temperature thus approaches zero and the density tends to infinity at the time $t_0 = (3\alpha\delta\nu_0)^{-1}$. From Eq. (26) it follows that the condition for runaway production $E_\parallel > E_c$ corresponds to

$$\frac{T(t)}{T_0} < \left(\frac{m_e c^2}{T_0}\frac{E_{\parallel 0}}{E_{D0}}\right)^{2/(3-\lambda/\delta)}. \tag{34}$$

We can now rewrite Eq. (30) for suprathermal electrons as

$$\frac{\partial F}{\partial s} + 3\alpha\delta F + \delta x\frac{\partial F}{\partial x} = \frac{1}{x^2}\frac{\partial}{\partial x}\left(F + \frac{1}{2x}\frac{\partial F}{\partial x}\right), \tag{35}$$

where the new time variable s is defined by $ds/dt = \hat{\nu}_{ee}$. Assuming that $\lambda/\delta \sim 1$ or smaller, Eq. (35) can be solved with asymptotic expansion in the same way as (11) was solved in Ref. 7. The solution has the same structure and consists of an asymptotic matching across five different regions in velocity space. To lowest order in δ, the asymptotic solution is the same as in Ref. 7 in the three lowest velocity regions. In region III ($x < \delta^{-1/3}$, $y < 1$), the logarithm of F is expanded as

$$\bar{F} = \ln(F) = \delta^{-2/3}(\bar{F}_0 + \delta^{2/3}\bar{F}_1 + \cdots), \tag{36}$$

and Eq. (35) becomes

$$\frac{\partial \bar{F}}{\partial \tau} + y\frac{\partial \bar{F}}{\partial y} + 3\alpha = \frac{1}{y^2}\left(1 - \frac{\delta^{2/3}}{2y^3}\right)\frac{\partial \bar{F}}{\partial y} + \frac{\delta^{2/3}}{2y^3}\left[\left(\frac{\partial \bar{F}}{\partial y}\right)^2 + \frac{\partial^2 \bar{F}}{\partial y^2}\right], \tag{37}$$

where $\tau = \delta s$. This equation differs from the corresponding region III equation in Ref. 7. Consequently, the density variation starts to play a role in region III and the solution is different from the one in Eq. (19). Solving the two lowest-order equations for $\bar{F}$, one obtains for $y < 1$ and $\tau \to \infty$

$$\bar{F}_0 \to -y^2 + \frac{2}{5}y^5, \tag{38}$$

$$\bar{F}_1 \to (\alpha - 1)\ln(1 - y^3), \tag{39}$$

so the asymptotic solution to Eq. (37) is

$$F_{III} = \lim_{\tau\to\infty} F = (1 - y^3)^{\alpha-1}\exp\left[-\delta^{-2/3}\left(y^2 - \frac{2y^5}{5}\right)\right]. \tag{40}$$

As in Ref. 7, the expansion in region III breaks down close to $x = \delta^{-1/3}(y = 1)$, and a boundary layer forms with the width $x - \delta^{-1/3} \sim 1$. In this boundary layer (region IV) around $x = \delta^{-1/3}$, Eq. (35) can be expressed in the new variable $r = x - \delta^{-1/3}$ to the lowest-order (δ^1) as

$$\frac{\partial F}{\partial \tau} + 3\alpha F + 3r\frac{\partial F}{\partial r} = \frac{1}{2}\frac{\partial^2 F}{\partial r^2}. \tag{41}$$

Equation (41), together with the requirement that $F \to 0$ as $r \to \infty$, has the asymptotic solution

$$F_{IV} = \lim_{\tau\to\infty} F = C_{IV}\exp(3r^2/2)D_{-\alpha}(r\sqrt{6}), \tag{42}$$

where $D_{-\alpha}$ is a parabolic cylinder function with the properties[17]

$$D_{-\alpha}(z) \to \begin{cases} \sqrt{2\pi}/\Gamma(\alpha)(-z)^{\alpha-1}e^{z^2/4}, & z \to -\infty \\ z^{-\alpha}e^{-z^2/4}, & z \to \infty. \end{cases} \tag{43}$$

Matching the $r \to -\infty$ limit of F_{IV} to the $y \to 1^-$ limit of F_{III} gives the constant C_{IV} in Eq. (42) as

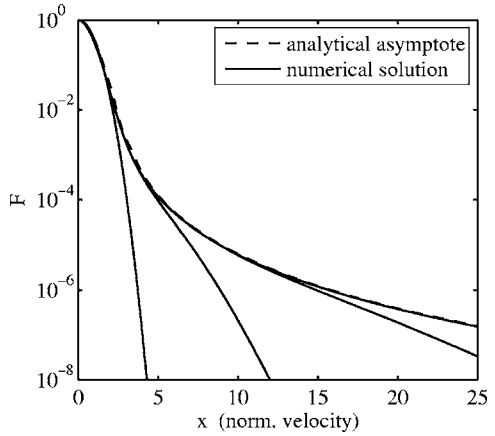

FIG. 10. (Dashed) the analytical asymptotic distribution function (46) as $t \to t_0$ for $\delta=\lambda=0.05$. (Solid) a numerical solution given at the times corresponding to the temperatures $T/T_0=1$, 10^{-1}, 10^{-2}, and 10^{-3} (from left to right).

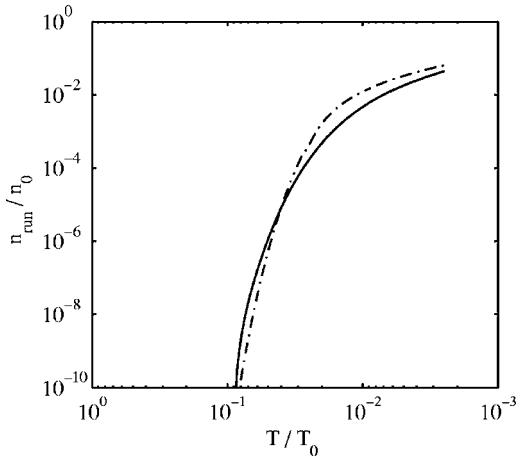

FIG. 11. Comparison of the analytical estimate in Eq. (47) for the runaway electron density (dash-dotted) with numerical solution (solid) when the temperature has fallen according to Eq. (33) to a fraction T/T_0 of the original temperature and the density follows Eq. (32). Here $E_{D0}/E_0=530$ and $\lambda=\delta=0.05$. The classical Dreicer generation predicts negligible amounts of runaways, since x_c [in Eq. (27)] does not decrease with time when $\lambda=\delta$.

$$C_{\mathrm{IV}}=\left(\frac{3}{2}\right)^{(\alpha-1)/2}\exp\left(-\frac{3}{5}\delta^{-2/3}\right)\frac{\Gamma(\alpha)}{\sqrt{2\pi}}. \tag{44}$$

In region V ($y>1$), Eq. (35) is to lowest order

$$\frac{\partial F}{\partial \tau}+3\alpha F+y\frac{\partial F}{\partial y}=\frac{1}{y^2}\frac{\partial F}{\partial y}, \tag{45}$$

and the asymptotic state is given by $F\to F_{\mathrm{V}}=C_{\mathrm{V}}(y^3-1)^{-\alpha}$. Finally, matching the $y\to 1^+$ limit of F_{V} to the $r\to\infty$ limit of F_{IV} to determine the constant C_{V} yields the total asymptotic solution

$$\lim_{t\to t_0}F(y,t)=\begin{cases}(1-y^3)^{\alpha-1}\exp\left[-\delta^{-2/3}\left(y^2-\dfrac{2y^5}{5}\right)\right], & y<1\\ (\sqrt{3}\delta^{1/3})^{\alpha-1}2^{-\alpha/2}\dfrac{\Gamma(\alpha)}{\sqrt{\pi}}\exp\left\{\left[\dfrac{3}{2}(y-1)^2-\dfrac{3}{5}\right]\delta^{-2/3}\right\}D_{-\alpha}[\sqrt{6}(y-1)\delta^{-1/3}], & y-1\sim\delta^{1/3}\\ (\sqrt{3}\delta^{1/3})^{2\alpha-1}2^{-\alpha}\dfrac{\Gamma(\alpha)}{\sqrt{\pi}}\exp\left(-\dfrac{3}{5}\delta^{-2/3}\right)\dfrac{1}{(y^3-1)^{\alpha}}, & y>1.\end{cases} \tag{46}$$

Note that $D_{-1}(r\sqrt{6})=\sqrt{\pi/2}\,\exp(3r^2/2)\mathrm{erfc}(r\sqrt{3})$, so with no density variation ($\lambda=0$, $\alpha=1$) we recover the result of Ref. 7. Figure 10 shows a comparison between this approximate asymptotic solution and a full numerical solution of Eq. (30).

The number of runaways can now be estimated when $\delta^{-1/3}<x_{\mathrm{c}}<x_{\mathrm{tail}}$ by

$$\begin{aligned}n_{\mathrm{run}}/n&=\frac{4}{\sqrt{\pi}}\int_{x_{\mathrm{c}}}^{x_{\mathrm{tail}}}F(x^2-x_c^2)dx+\frac{4}{\sqrt{\pi}}\frac{n_0}{n}\\&\quad\times\int_{v_{\mathrm{tail}}/v_{T0}}^{\infty}e^{-x^2}\left(x^2-\frac{v_c^2}{v_{T0}^2}\right)dx\\&\simeq\frac{4}{\pi}(\sqrt{3}\delta^{1/3})^{2\alpha-1}2^{-\alpha}\Gamma(\alpha)\exp\left(-\frac{3}{5}\delta^{-2/3}\right)\\&\quad\times\left[\frac{1}{\lambda}(x_c^{1-\alpha}-x_{\mathrm{tail}}^{1-\alpha})-\frac{x_c^2\delta^{-\alpha}}{3\alpha-1}(x_c^{1-3\alpha}-x_{\mathrm{tail}}^{1-3\alpha})\right]\\&\quad+\frac{2}{\sqrt{\pi}}\frac{n_0}{n}\delta^{1/3}\exp(-\delta^{-2/3}).\end{aligned} \tag{47}$$

This estimate is compared in Fig. 11 with a numerical solution of Eq. (30) and with Dreicer runaway generation (17). The runaway burst is smaller than in the case of constant density, see Fig. 2, but now very much larger than Dreicer generation, which hardly produces any runaways because of the density dependence of the critical velocity through the Dreicer field. Of the three effects discussed at the beginning of this section, it is the second one (increasing x_{c}) that is responsible for turning off Dreicer production, while the

third one (higher collision frequency) reduces the runaway burst. A similar conclusion follows from inspecting numerical results with other cooling histories. Runaway bursts are not as sensitive to a density increase as the Dreicer mechanism.

The criterion given in Eqs. (23) and (24) for when the burst is more important than Dreicer generation is still valid when the density increases since region III (where the tail starts to deviate strongly from a Maxwellian) appears at the same place, $x \sim \delta^{-1/3}$.

VII. CONCLUSIONS

Our analysis confirms the conclusion previously made in the context of pellet injection simulations[4,5] that a high-energy tail forms in the electron distribution function in a rapidly cooling plasma and that this tail can easily be converted into a burst of runaway electrons. This mechanism can be more efficient than ordinary Dreicer generation, and could be very important during tokamak disruptions unless there are large and rapid losses of fast electrons. Equations (23) and (24) give an approximate criterion for whether runaway bursting is more important than Dreicer production, and suggest that this is indeed the case in large tokamak disruptions.

It is, however, difficult to predict the exact size of the runaway burst in a disruption since it is sensitive to several quantities that are poorly diagnosed, such as details of the density and temperature evolution. The runaway burst is reduced if the electron density increases during the thermal quench, for instance, by ionization of impurity atoms. However, ordinary Dreicer production is still more sensitive to a density increase, which thus makes the runaway burst relatively more important. In a future reactor-scale device such as ITER, its most important role could be to provide a seed population of fast electrons for a secondary runaway avalanche.[3]

ACKNOWLEDGMENTS

This work was funded jointly by the United Kingdom Engineering and Physical Sciences Research Council and by the European Communities under Association Contracts between EURATOM, the Swedish Research Council, UKAEA, and CEA Cadarache. The views and opinions expressed herein do not necessarily reflect those of the European Commission.

[1] J. W. Connor and R. J. Hastie, Nucl. Fusion **15**, 415 (1975).
[2] R. H. Cohen, Phys. Fluids **19**, 239 (1976).
[3] M. N. Rosenbluth and S. V. Putvinski, Nucl. Fusion **37**, 1355 (1997).
[4] S. C. Chiu, M. N. Rosenbluth, R. W. Harvey, and V. S. Chan, Nucl. Fusion **38**, 1711 (1998).
[5] R. W. Harvey, V. S. Chan, S. C. Chiu, T. E. Evans, M. N. Rosenbluth, and D. G. Whyte, Phys. Plasmas **7**, 4590 (2000).
[6] P. L. Taylor, A. G. Kellman, T. E. Evans, D. S. Gray *et al.*, Phys. Plasmas **6**, 1872 (1999).
[7] P. Helander, H. Smith, T. Fülöp, and L.-G. Eriksson, Phys. Plasmas **11**, 5704 (2004).
[8] M. Bakhtiari, Y. Kawano, H. Tamai, Y. Miura, R. Yoshino, and Y. Nishida, Nucl. Fusion **42**, 1197 (2002).
[9] D. J. Ward and J. A. Wesson, Nucl. Fusion **32**, 1117 (1992).
[10] P. Helander and D. J. Sigmar, *Collisional Transport in Magnetized Plasmas* (Cambridge University Press, Cambridge, 2002).
[11] H. Dreicer, Phys. Rev. **115**, 238 (1959); **117**, 329 (1960).
[12] L. D. Landau and E. M. Lifshitz, *Quantum Mechanics*, Course of Theoretical Physics Vol. 3, 3rd ed. (Pergamon, Oxford, 1977).
[13] V. Riccardo and JET EFDA contributors, Plasma Phys. Controlled Fusion **45**, A269 (2003).
[14] R. Aymar, P. Barabaschi, and Y. Shimomura (for the ITER Team), Plasma Phys. Controlled Fusion **44**, 519 (2002).
[15] ITER Physics Basis, Nucl. Fusion **39**, 2137 (1999).
[16] L-G. Eriksson and P. Helander, Comput. Phys. Commun. **154**, 175 (2003).
[17] M. Abramowitz and I. J. Stegun, *Handbook of Mathematical Functions* (Dover, New York, 1974).